Friction-based dissipative devices for precast concrete panels

Bruno Dal Lago *, Fabio Biondini, Giandomenico Toniolo

Department of Civil and Environmental Engineering, Politecnico di Milano, Piazza Leonardo da Vinci 32, 20133 Milan, Italy

The stability of precast concrete wall panels under seismic action can be ensured by means of dissipative systems of panel-to-panel connections that allow to control the level of forces and limit the displace-ments. This paper deals with a connection system consisting of friction-based devices inserted into appropriate recesses within the joints between vertical or horizontal panels. The results of experimental tests carried out on single connectors, as well as on structural sub-assemblies consisting of two full scale panels, are presented. The technological choices of materials and components that ensure a stable hysteretic behaviour of the devices are discussed. The effectiveness of the devices in improving the seismic performance of precast buildings under seismic action is also shown based on the results of cyclic and pseudo-dynamic tests on full-scale structural prototypes.

Keywords:
Precast structures
Concrete panels
Dry-friction connections
Energy dissipation
Experimental testing

1. Introduction

In the last two decades, relevant research advances supported by extensive experimental activities and theoretical studies have been accomplished in the field of seismic design of precast structures [1–7]. Moreover, a well-established framework of design rules for precast concrete systems is incorporated in seismic design codes [8]. However, some issues concerning the seismic behaviour of precast buildings with cladding wall panels are still open, and adequate technological solutions and effective design rules for this type of structures are not yet implemented in current design practice. The limitations of the current design approach have been shown during recent earthquakes in Southern Europe by several structural failures of cladding precast panels due to the inadequate behaviour of the fastening connection systems [9–13].

A research activity has been carried out at European level within the SAFECLADDING project [14] to provide guidelines for a proper seismic design of precast structures with cladding panels and to propose innovative systems of connections. In particular, the use of dissipative connection devices can ensure the stability of the cladding panels under seismic action and improve the seismic performance of the earthquake resisting system by providing energy dissipation capacity under controlled forces and limited displacements [15,16].

Friction Based Devices (FBDs) are mechanical connections inserted into appropriate recesses within the joints between vertical or horizontal concrete panels. They provide dissipation of energy when subject to imposed displacement. An interesting application of this type of device refers to precast structures. Typical precast frame systems are very flexible and provided with stiff concrete cladding wall panels that in current design practice are supposed not to interact with the structure. If the panels are connected to the frame structure by means of statically determined schemes, the use of FBD panel-to-panel dissipative connections make the whole façade much stiffer and integral part of the earthquake resist-ing system up to the force associated with the friction threshold of the devices.

This type of connection, which usually includes brass sheets to stabilise the hysteretic cycles, can be also considered as a Brass Friction Device accordance to the classification proposed by Schultz et al. [17]. Several other examples of friction-based connec-tors can be also found in literature [18–23], including for use in precast structures [24,25].

The basic configuration of the FBD has been investigated in [15,26] and further developed in [27–28]. This paper presents the results of experimental tests carried out on single FBD connectors, as well as on structural sub-assemblies consisting of two full scale panels with multiple connectors. Emphasis is given to the technological choices of materials and components that ensure a stable hysteretic behaviour of the FBD devices. The results of cyclic and pseudo-dynamic tests on full-scale structural prototypes are also presented to show the effectiveness of the devices in improving the seismic performance of precast buildings under seismic action.

2. Friction-based device

The FBD is made by three elements assembled through bolts, as shown in Fig. 1:

* Corresponding author.
E-mail address: brunoalberto.dallago@polimi.it (B. Dal Lago).

©2017. This manuscript version is made available under the CC-BY-NC-ND 4.0 license http://creativecommons.org/licenses/by-nc-nd/4.0/
Published Journal Article available at: http://dx.doi.org/10.1016/j.engstruct.2017.05.050

- *Support profile*, made of mild steel, which connects the device to the concrete panel. The support profile can be T-shaped (Fig. 1a), to obtain a symmetric device-to-panel connection, or L-shaped, for an asymmetric connection. The component is provided with vertical slots, that allow for the relative displacement between the two adjacent support profiles, and with holes or short horizontal slots on the panel side for a bolted device-to-panel connection, or for temporary support of a welded device-to-panel connection. A symmetric profile, e.g. T-shaped, can be symmetrically connected with the panel side, leading to a distribution of forces that avoids any torsion. It requires the assemblage to be made from two sides, in order to tighten all the bolts. An asymmetric profile, e.g. L-shaped, allows the assemblage to be performed from one side only (for cladding panels, generally the inner side of the building). It leads to additional torsional force components in the panel connection.
- *Brass sheet*, provided with two vertically aligned round holes in one side and with two vertically aligned horizontal slots in the other side (Fig. 1a). Two brass sheets connect the support profiles through bolts, providing also a horizontal mounting tolerance which is related to the length of the slots. If the support profiles are forced to mutually slide, friction occurs between the brass sheets and the support profiles.
- *Cover plate*, made of mild steel, having the same geometry of the brass sheet (Fig. 1a). A steel plate covers each brass sheet to avoid its out-of-plane deformation and ensure the correct kinematic of the connection.

Fig. 1b shows an assembled connection with symmetric T-shaped support profiles. Brass sheets and cover plates can be mounted in mirrored or inverted configuration. Fig. 1c shows the axonometric view of the connection with inverted plates. The mirrored configuration yields to a symmetric distribution of forces up to the sliding shear threshold, after which all horizontal reactions due to shear increments coming from the rotational equilibrium of the plates are taken by the support profile adjacent to the round holes of the plates. The inverted configuration always provides a symmetric distribution of forces and is suggested to be adopted.

The connection can be pre-assembled by mounting two support profiles, two brass sheets and two cover plates with bolts, nuts and washers without tightening: it is placed in position between the panels, adjusted and then tightened. Alternatively, the connection can be assembled in site with each component at a time.

Fig. 2 shows the assembled device in the undeformed configuration (Fig. 2a) and under imposed relative displacement (Fig. 2b). Fig. 3 provides a technical drawing of the components of the connection. The maximum displacement allowed by the connection is equal to the length L_v of the vertical slots of the support profile, regardless of the position of installation of the bolts. The installation tolerance in the vertical direction is hence provided by these slots. Horizontal in-plane tolerance is provided by the horizontal slots on brass and steel plates with length L_h. The horizontal out-of-plane tolerance is provided by holes or slots on the support profile.

3. Tests on single devices

The tests on single devices have been carried out on a uniaxial ± 1000 kN Schenck machine at the Laboratorio Prove e Materiali of Politecnico di Milano through the application of vertical displacement histories (Fig. 2).

3.1. Test setup and experimental program

The connection is attached through bolts to two opposite strong L-shaped support elements made of two HEA steel profiles welded together and fixed to the machine through thick steel plates provided with large diameter bolts. In addition to the standard machine instrumentation, two ±150 mm displacement transducers have been installed with magnetic bases in order to measure the exact drift between the L-shaped profiles. Two ±5 mm Gefran displacement transducers have also been placed vertically attached to the support elements. The results presented in the following are cleared from the millimetric movements of the support profiles recorded by those transducers.

Monotonic tests are performed with a constant speed of 0,25 mm/s. Three different cyclic protocols have been applied with a constant speed of 2 mm/s:

- Protocol I consists of constant displacement amplitudes of ±20 mm repeated ten times.
- Protocol II consists of constant displacement amplitudes of ±40 mm repeated ten times.
- Protocol III consists of increasing displacements with amplitudes: 2,5–5–10–20–40 mm. Each amplitude is cycled three times.

The cyclic tests carried out on single connections are listed in Table 1. The tests have been performed with the aim to set up the best configuration of the device and to investigate several technological issues, both regarding the performance of the connection and its operability. These issues include:

- The necessity of using the brass plates;
- The efficiency of sandblasting surface treatment, aimed at increasing the steel-brass friction coefficient;
- The possibility of re-use of the same components after several cycles;
- The behaviour using different types of washers;
- The behaviour using symmetric or asymmetric support profiles.

Additional issues have been explored, including the influence of the speed of the test and the need to control the torque. Cyclic tests performed with a reduced speed of 0,1 mm/s yielded very similar results with respect to those performed at full speed. The use of a dynamometric wrench could increase the installation cost of the connection. However, as clearly shown by the test results with different applied torque, the axial force given to the bolts through tightening is directly related to the slip load threshold.

3.2. Use of brass sheets

The use of brass sheets is of economical concern for the device, since these components represent a relevant portion of the total cost of the device. In the device without brass sheets sliding occurs between the steel surfaces of the support profile and the cover plate with a steel-steel friction. Figs. 4a and b show the load vs displacement diagrams of specimens provided with and without brass sheets, respectively. By comparison, it can be noted that a cyclic instability occurred in the case without brass sheets, since the slip load significantly increases with large drifts causing plastic deformation of the support profile, as shown in Fig. 4c. This happened because of the blocking of the steel surfaces, due to a "mechanical welding" effect. None of the performed tests with the traditional configuration of a brass friction device showed this cyclic instability, suggesting that brass sheets are necessary to stabilise the hysteretic behaviour of the device.

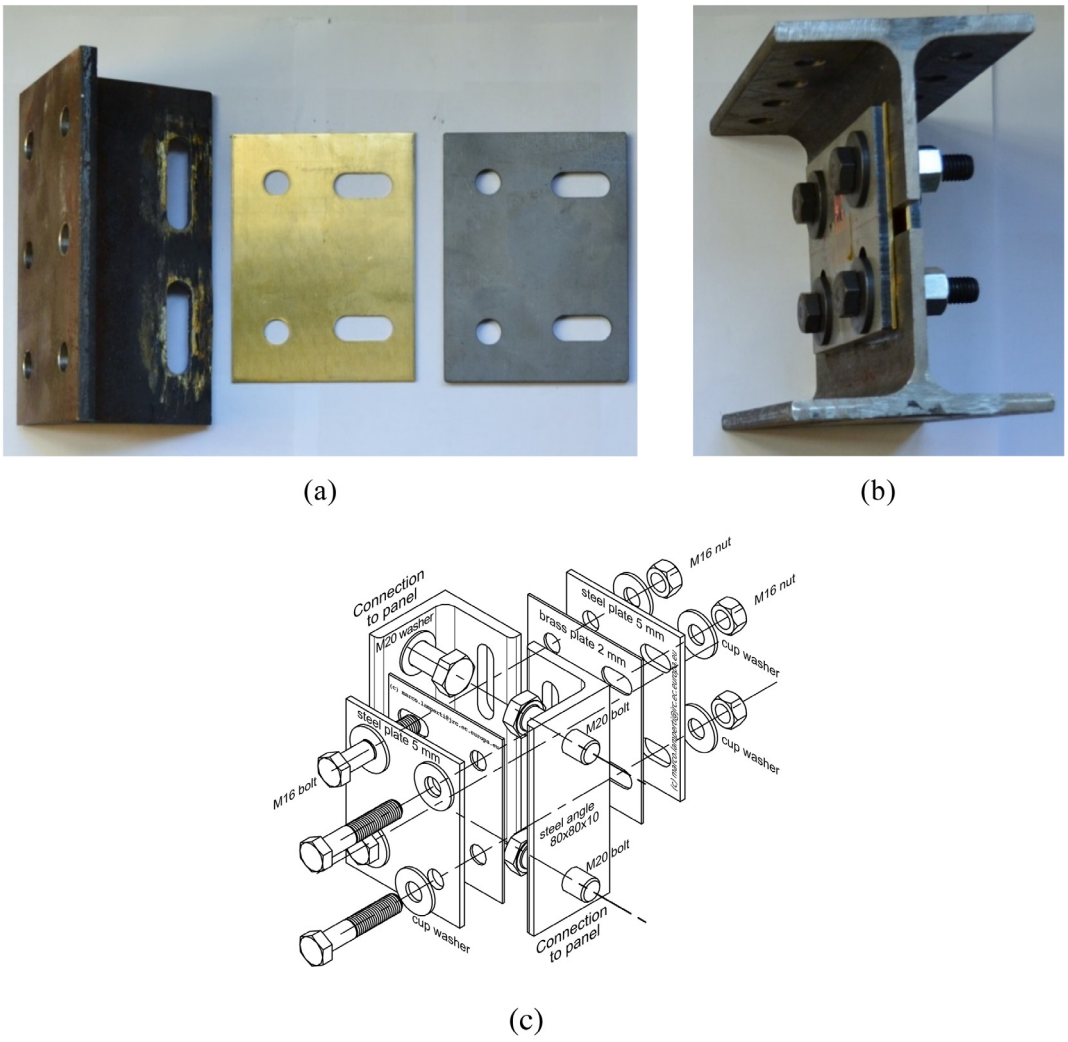

Fig. 1. Friction Based Device (FBD): (a) components, (b) device assembled on T-shaped supports, and (c) axonometric view of the device on L-shaped support profiles with inverted plate configuration (courtesy of M. Lamperti Tornaghi).

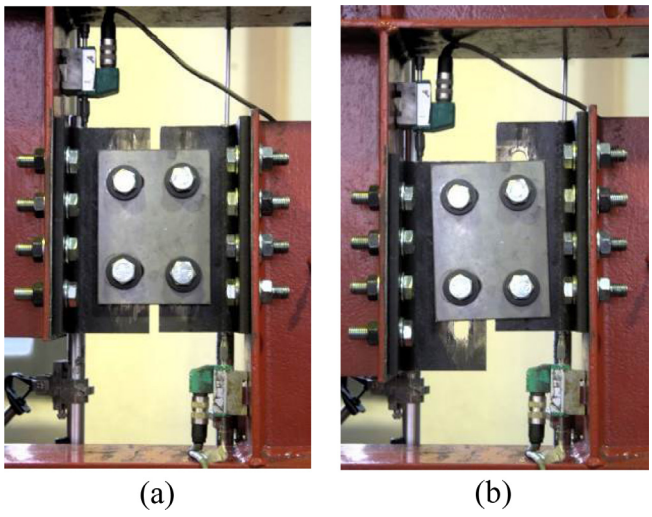

Fig. 2. Test setup: FBD (a) assembled and (b) subjected to maximum drift.

3.3. Effect of sandblasting surface treatment

Sandblasting surface treatment has been applied to both the inner sides of the brass sheets in order to increase the friction coefficient between steel and brass, trying to maximize the slip load threshold. The comparison of the cyclic behaviour reported in Figs. 5a and b shows that the surface treatment is efficient in increasing the slip load threshold. However, the results show that this effect is strongly active only for monotonic loading, since after the first semi-cycle the behaviour quickly tends to that of a specimen provided with ordinary brass sheets. This is due to the abrasion of the sandblasting, that occurs very soon.

Fig. 6 shows the comparison between a sandblasted and an ordinary brass sheet after a tests with protocol I. The sandblasted surface is strongly abraded, exposing the underneath smooth surface. It can be concluded that sandblasting is not effective in improving the hysteretic behaviour of the device.

3.4. Re-use of the connection

The global cost of the connection shall take into account the operations and substitutions that need to be done after service use to make the connection fully operative again. In particular, special attention has been dedicated to the re-use of the brass sheets, since they are subjected to abrasion during the motion (Fig. 7a) and they also represent a large part of the connection global cost. Several tests have then been repeated twice using the same components (Fig. 7b), without dismounting the connection and with the

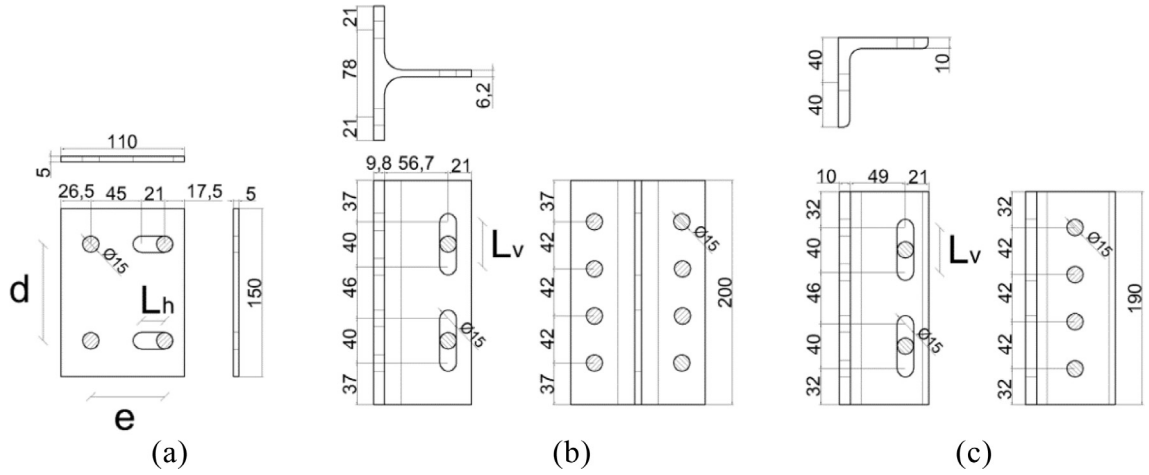

Fig. 3. Geometry of (a) steel cover plates, (b) T-shaped support profile, and (c) L-shaped support profile (mm).

Table 1
List of tests performed on single FBDs.

Test ID	Load protocol	Specimen	Speed [mm/s]	Support shape	Bolts	Torque [Nm]	Washer
L-1	I	New	0,1	T	8.8	134	THIN
L-2	I	Used	0,1	T	8.8	134	THIN
L-3	I	Used	2,0	T	8.8	134	THIN
L-4	I	New	2,0	T	8.8	134	THIN
L-5	I	Sandblasted 1	2,0	T	8.8	134	THIN
L-6	I	Sandblasted 2	2,0	T	8.8	134	THIN
L-7	I	Reversed	2,0	T	8.8	134	THICK
L-8	I	New	2,0	T	8.8	134	THICK
L-9	II	New	2,0	T	8.8	80	THICK
L-10	II	Used	2,0	T	8.8	134	THICK
L-11	II	New	2,0	T	8.8	134	ELASTIC
L-12	II	New	2,0	T	8.8	134	BELLEVILLE
L-13	II	New	2,0	T	10.9	190	BELLEVILLE
L-14	II	Reversed (new)	2,0	T	10.9	190	BELLEVILLE
L-15	II	Reversed (used)	2,0	T	10.9	190	BELLEVILLE
L-18	II	Angles (new)	2,0	L	10.9	190	BELLEVILLE
L-19	II	Angles (used)	2,0	L	10.9	190	BELLEVILLE
L-20	III	New	2,0	T	8.8	134	THICK
L-21	III	New	2,0	T	8.8	134	ELASTIC
L-22	III	New	2,0	T	8.8	134	BELLEVILLE
L-23	III	New	2,0	T	10.9	190	BELLEVILLE
L-24	III	Used	2,0	T	10.9	190	BELLEVILLE
L-25	III	Reversed (no brass)	2,0	T	10.9	190	BELLEVILLE
L-28	III	Angles (new)	2,0	L	10.9	190	BELLEVILLE
L-29	III	Angles (used)	2,0	L	10.9	190	BELLEVILLE

only operation of re-tightening. The comparison between the hysteretic cycles of a used connection (Fig. 7b) and a new one (Fig. 4a) shows that the performance of the connection is not substantially influenced by its previous strong abrasion. Similar results have been obtained with all tests repeated with new and used specimens. Thus, it is possible to state that the components of the connection can be re-used after a strong motion without the need of substitution of whichever component. However, re-tightening is needed in order to restore the original axial load in the bolts, which could have lowered due to abrasion of the brass sheet and consequent bolt shortening with axial load losses.

3.5. Use of different types of washer

A comparison among specimens provided with different types of washers shows that this component can have a large influence on the cyclic response of the connection. Four different types of washers have been considered, from normal thin M14 washers to thick M14 washers, up to improved types of washers such as elastic (spiral-shaped cut washers) and Belleville (with spherical shape). The hysteretic cycles of the specimen with standard thin washers (Fig. 5a) show a large loss of dynamic load slip threshold through the cycles, with a lowering that reaches about 20 kN within the second and the third cycles. At the end of the test, the residual axial load in the bolts has been approximately measured by using the mechanical wrench for unscrewing. The initial applied tightening torque was of 134 Nm. At the only side subjected to slippage, a residual tightening torque of less than 50 Nm, the minimum allowed by the wrench, has been measured for both the bolts, while a higher residual tightening torque of about 100 Nm has been measured for the bolts of the side not subjected to slippage. The specimen with thick washers also shows large losses, reaching a slip threshold of about 20 kN within the second and third cycles. Residual tightening torques have been measured equal to 60–70–70–100 Nm on the four bolts.

Some improvements can be noticed in the specimen provided with elastic washers (Fig. 8a), with which three to four cycles can develop before the slip threshold lowers down to 20 kN. Residual tightening torques of 50–90–90–110 Nm have been measured.

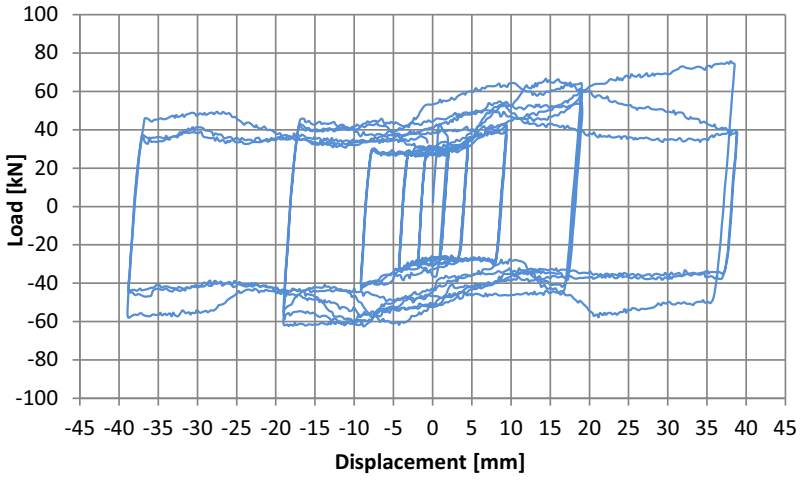

(a)

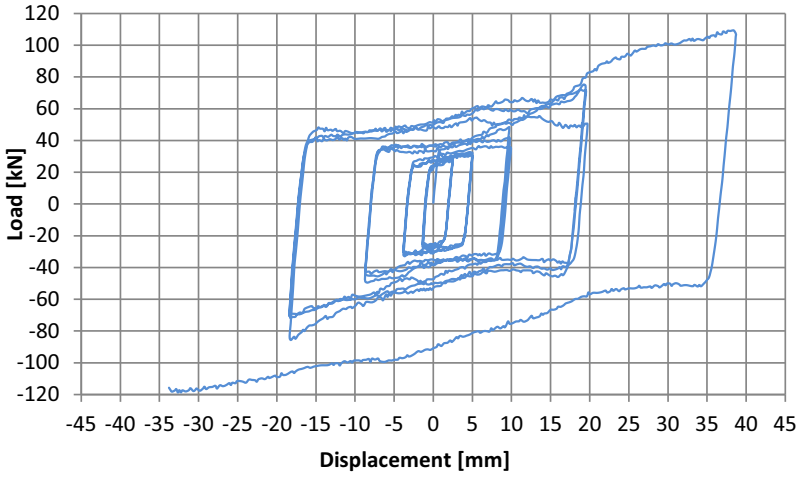

(b)

(c)

Fig. 4. Effect of brass sheets: (a) load vs displacement diagram for specimen provided with brass sheet (L-23), (b) load vs displacement diagram for specimen without brass sheet (L-25) and (c) picture of one support profile at the end of the test without brass sheet (L-25).

The best performance is obtained with the specimen equipped with Belleville washers (Fig. 8b). Also this solution shows a tendency to lower the slip threshold, but reducing losses in such a way that the slip threshold remains at about 30 kN also after the full sequence of ten large displacement cycles. The residual tightening torques that have been measured are equal to 70–11 0–110–110 Nm. The losses observed in all cases are due to the abrasion of the brass sheet. The bolts are tightened within a short length, between 24 and 28 mm in the performed tests, and thus a surface abrasion of several hundredths of millimetre can cause a shortening in the bolt that corresponds to a strong loss. The elongation of a bolt having 28 mm of clear distance between the nuts tightened at 400 MPa is in fact equal to only 0,053 mm, if considering an elastic modulus of 210 GPa. Traditional flat washers do not provide a restraint for the bolt shortening, but improved washers, such as elastic and Belleville, are aimed to keep the pre-load even under small shortening, as per their elastic stiffness. A slight increase of the elastic stiffness of the overall connection with stiffer washers is also noticed, from a value of about 40 kN/mm with thin washers, to 45 kN/mm with thick washers, 50 kN/mm with elastic washers, and 55 kN/mm with Belleville washers.

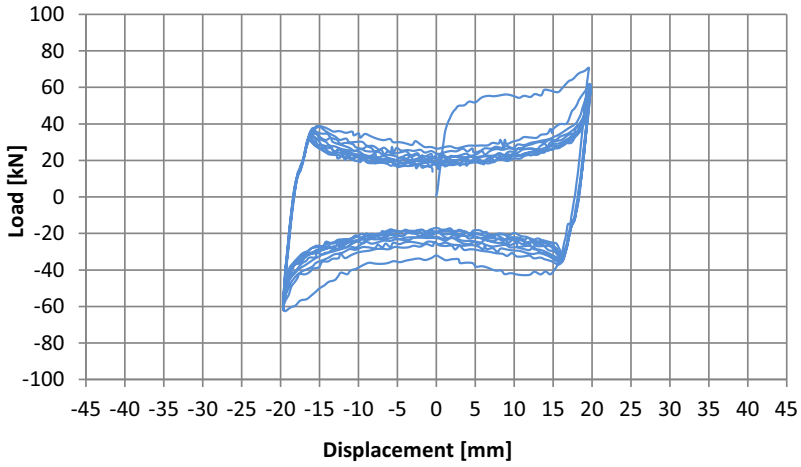

(a)

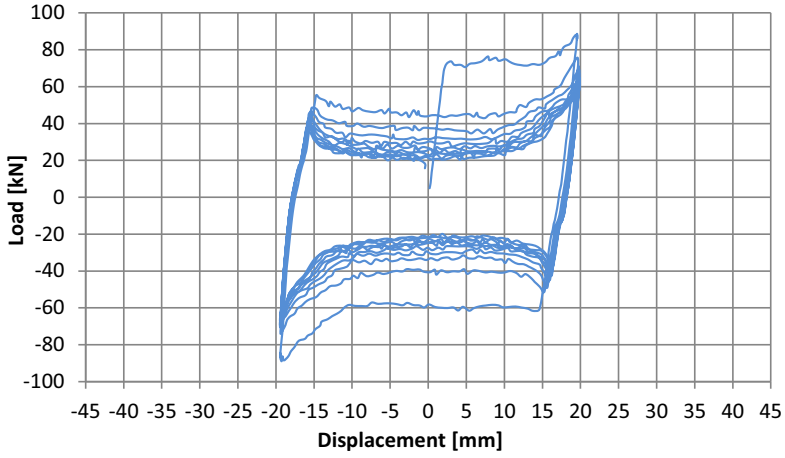

(b)

Fig. 5. Effect of sandblasting: load vs displacement diagram for (a) specimen with untreated brass sheets (L-3) and (b) specimen with inner sandblasted brass sheets (L-5).

(a) (b)

Fig. 6. Brass sheets after testing: (a) untreated (L-3) and (b) sandblasted (L-5).

3.6. Asymmetric support profiles

Several tests have been performed on the connection attached to asymmetric support profiles, that allow to mount and dismount the connection from one panel side only. Thick angle profiles have been used with the final technological configuration coming from previous tests, with Belleville washers and untreated brass sheets. M14 class 10.9 bolts are used and tightened at 190 Nm. Fig. 9a shows the load vs displacement diagram of this specimen tested with protocol II. A large cyclic stability is observed. Similar results are obtained with used components. The tests performed with protocol III also exhibit a large cyclic stability and dissipation properties, as shown in Fig. 9b, both for new and used specimens.

4. Panel sub-assembly tests

An experimental campaign on panel sub-assembly systems has been carried out at the Laboratorio Prove e Materiali of Politecnico di Milano in order to investigate the behaviour of both single devices and groups of joint connections when subjected to sliding between concrete panels, as well as to check the fastening of the support profiles to the wall panels.

The test setup is illustrated in Fig. 10a. It consists of of two solid concrete panels 129 cm large, 323 cm long and 16 cm thick, with aspect ratio equal to 2,50. The panels are provided with a top vertical slot at mid-width for the installation of the panel-to-beam connection, with a distance from the bottom panel-to-foundation connection to the top panel-to-beam connection of 280 cm. Three

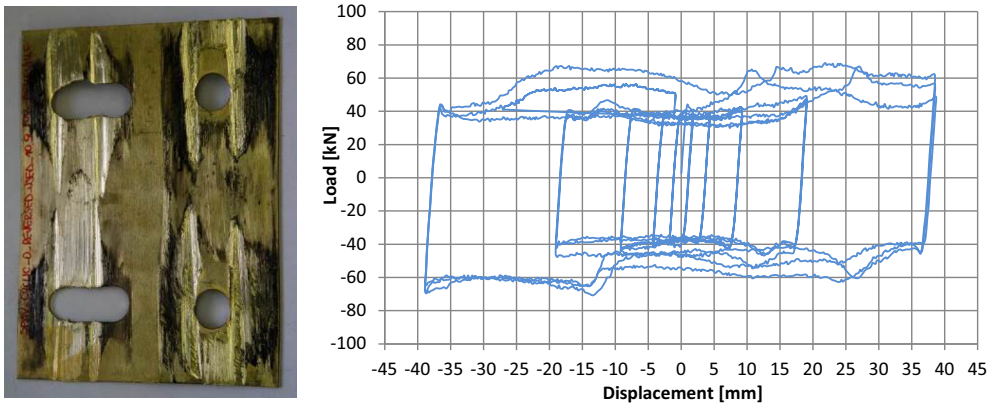

(a) (b)

Fig. 7. Re-use of the same components: (a) brass sheet after test (L-23), (b) load vs displacement for specimen with used components (L-24).

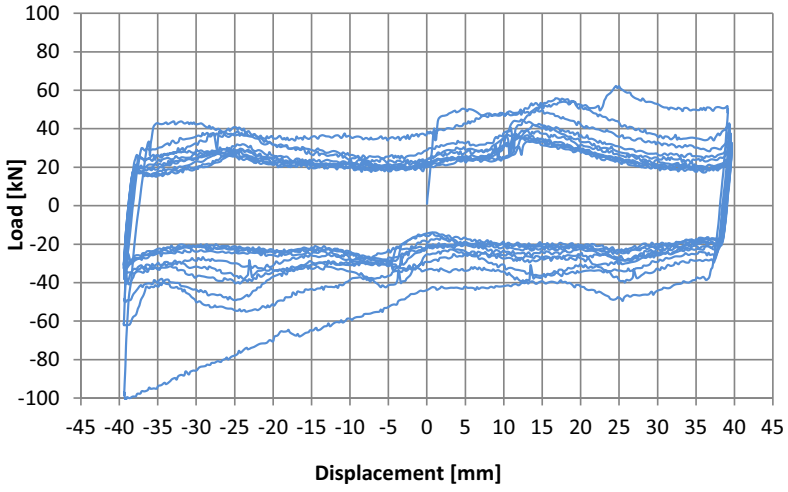

(a)

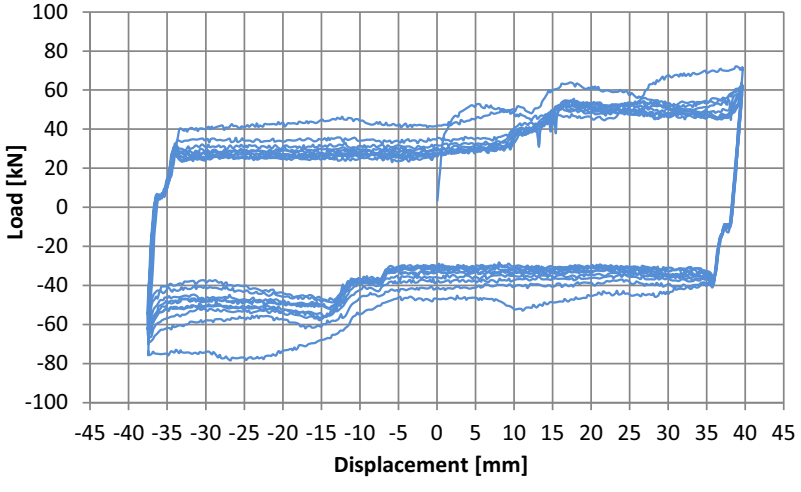

(b)

Fig. 8. Effect of different type of washers: load vs displacement for (a) specimen with elastic washers (L-11) and (b) specimen with Belleville washers (L-12).

recesses are placed at the thirds of this distance to host the dissipative connections. The base panel connection is made with a pin inserted into a steel fork bolted to sockets embedded into the panel and to the foundation beam. The top panel connections are made of passing round holes hosting steel pins that connect the panels to the steel articulated frame that transmits the imposed displacements to the panels (Fig. 10b). The frame is made of two HEA columns hinged at the bottom to the strong base steel beam

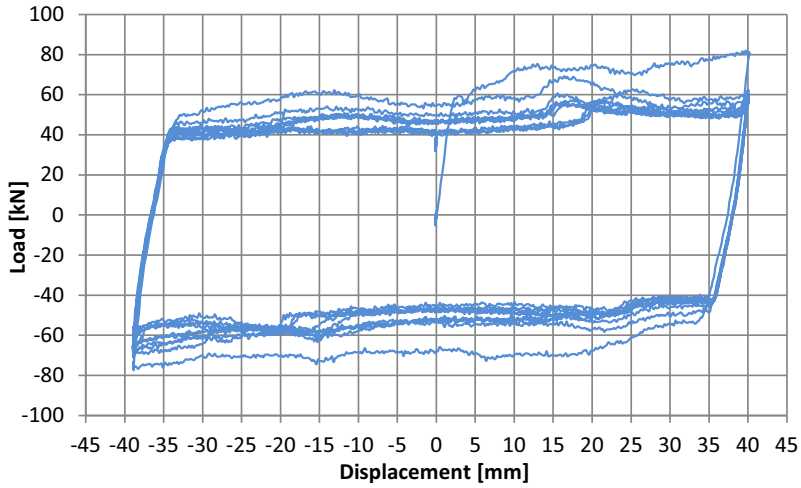

(a)

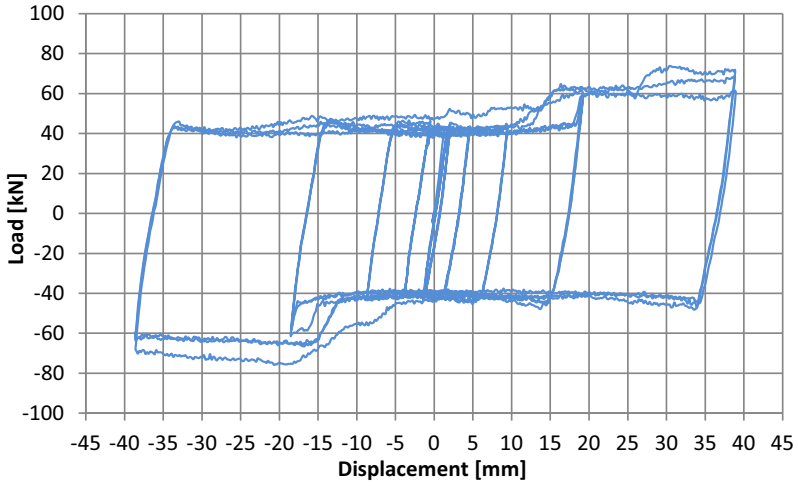

(b)

Fig. 9. FBDs with angle support profiles: load vs displacement diagrams for (a) constant amplitude protocol (L-18) and (b) increasing amplitude protocol (L-29).

and at the top to the double UPN beam that includes the panels. All hinges are made by steel pins. The frame is connected with the horizontal 750 kN jack, which is fixed to the strong steel reaction frame with the centre at a height of 285 cm. A lateral displacement retainer system has been attached to the top beam with steel spheres that are fixed to lateral stiff retaining frames.

Two vertical long slots are made in the beam UPN profiles in order to insert the panel-to-beam connection pins. The panel-to-foundation connection is also pinned. The whole system is designed to apply displacement histories with a negligible stiffness of the test setup, thus indirectly applying the load to the dissipative connections interposed in between the panels. Fig. 10c shows a picture of the assembled setup. This connection arrangement, which could also be used for full-scale cladding panels in real applications, would require a U-shaped profile to be embedded in the panel foundation to keep the room for the expected rotation of the panel.

The test instrumentation, in addition to the main displacement transducer that provides the control of the jack and load cell, consists of vertical displacement transducers placed at the panel base edges and connected to the base steel beam. Displacement transducers are installed on the concrete panels to measure their relative vertical sliding and horizontal movement.

Cyclic tests with protocols II and III, adapted to the geometry of the setup by amplifying the displacements by the panel aspect ratio, have been performed with specimens provided with one, two and three connections at the panel joints. The list of the performed sub-assembly tests is reported in Table 2.

The recesses in the panels have been designed in order to accommodate the FBDs made with symmetric T-shaped profiles and class 10.9 M14 bolts provided with Belleville washers. The support profile-to-panel connection is bolted, with six 8.8 M16 bolts that connect the profile with a steel counter-plate provided with sockets and with a bull horn bent Φ20 B450C rebar welded in its vertical portion to the counter-plate. Fig. 11 shows the sub-assembly under testing (Fig. 11a) and a detail of a displaced FBD connection (Fig. 11b). In the tests with single connection, the device was installed in the central recess. In the test with two con-nections, the devices were installed at the top and bottom recesses. The choice of the installation position, however, is not so relevant, since the panels tend to act as rigid bodies during the motion.

The experimental results in terms of load vs vertical relative displacement of the panels are shown in Fig. 12a for the tests performed with protocol II and in Fig. 12b for the tests performed with protocol III.

The cyclic behaviour of the sub-assembly tests (Fig. 12) is in accordance with the results of the local tests on the same device

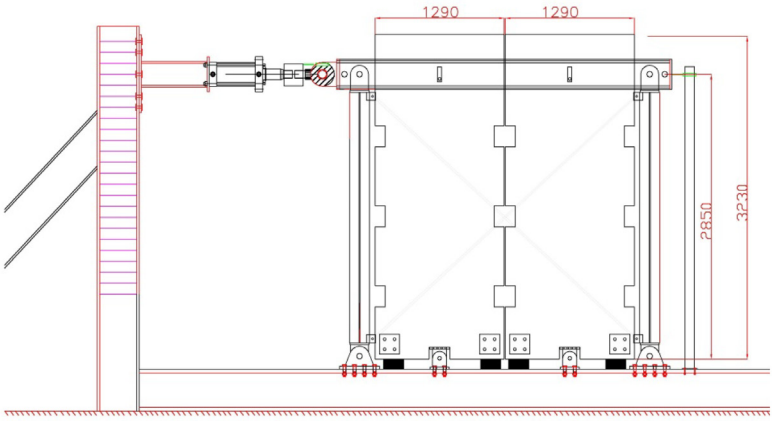

(a)

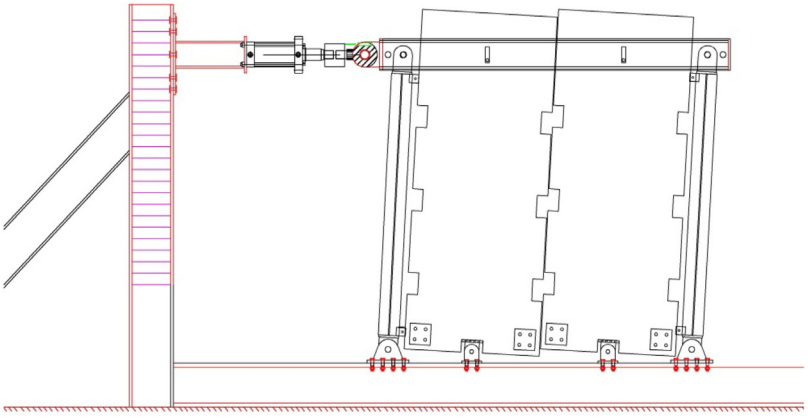

(b)

(c)

Fig. 10. Setup for panel sub-assembly tests: (a) geometrical dimensions (mm), (b) kinematics of the panels, and (c) view of the assembly.

(see Fig. 9). The experimental elastic stiffness calculated on the basis of the local tests multiplying the load by the panel aspect ratio is about 120 kN/mm for the specimen with three FBDs, about 80 kN/mm for the specimen with two FBDs and about 40 kN/mm for the specimen with one FBD.

For what concerns the slip threshold load attained, it is clear from the results of the tests with protocol III that the intrinsic uncertainty of the friction mechanism can cause relevant variations from the expected values. In particular, for this case the test with three and two devices show very similar results despite the

Table 2
List of the sub-assembly tests performed on concrete panels with FBDs.

Test ID	No. of devices	Load protocol	Bolts	Torque [Nm]	Washer
S-1	1	II	10.9	190	Belleville
S-2	1	III	10.9	190	Belleville
S-3	2	II	10.9	190	Belleville
S-4	2	III	10.9	190	Belleville
S-5	3	II	10.9	190	Belleville
S-6	3	III	10.9	190	Belleville

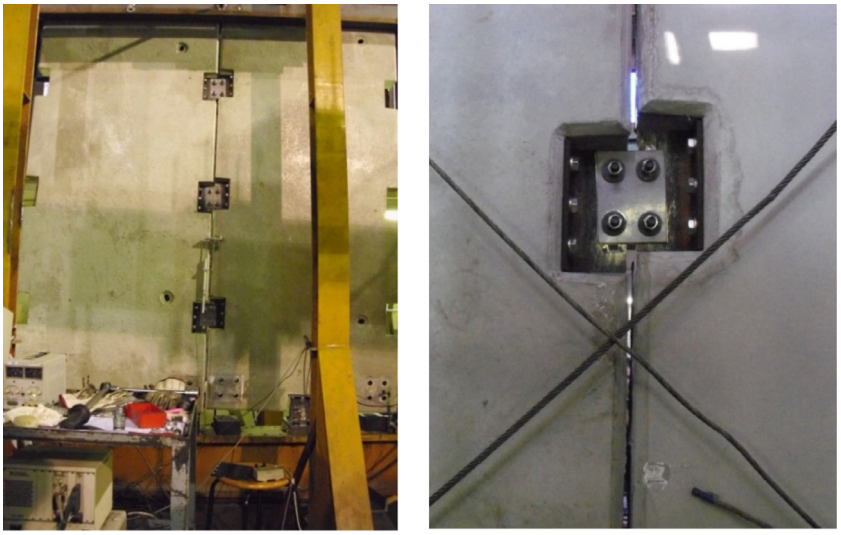

Fig. 11. Panel sub-assembly tests: (a) elevation view of the displaced panels and (b) detail of one connection subject to large drift.

different numbers of connections. A relevant level of uncertainty is typical of friction phenomena (details on the friction mechanics can be found in [29]). This uncertainty is taken into account in the design rules for the device proposed in this paper.

The elasticity of the structural sub-assembly also plays a role in the experimental response. It can be noted from the diagrams in Fig. 12 that the specimens with one connection only had a relative joint slide about two millimetres larger than the one with two connections and about four millimetres larger than the one with three connections, despite the fact that the displacement history applied at the top of the panels was the same. This phenomenon may slightly affect the global hysteresis of the system with a pinching effect limited to the small elastic deformations of the structure and its connections.

5. Full-scale prototype tests

An experimental campaign on a full-scale prototype of a precast structure has been performed at the ELSA laboratory of the Joint Research Centre of the European Commission in Ispra (Italy) in cooperation with Politecnico di Milano. The precast frame prototype represents a typical structure for industrial buildings and it has been designed at ultimate limit state (ULS) with peak ground acceleration $a_{g,max}$ equal to 0,36 g according to Eurocode 8 [8]. The aim of the experimental campaign, performed within the scope of the European research project Safecladding [14], has been to test different connection arrangements of both vertical and horizontal cladding panels, including arrangements with dissipative connections. The precast frame structure had one 5-m single bay and two 8-m spans. Each of the six 500-by-500 mm square-section cantilever columns was reinforced with 8 Φ24 at cross-section corners and mid-sides, surrounded by Φ12 stirrups spaced by 80 mm. Their clear height protruding from the pocket foundation was 7 m. Rectangular cross-section solid elements were used for the four 750-by-500 mm beams and for the seven 2350-by-350 mm roof elements. Concrete class C45/55 and reinforcing steel grade B450C were used for all elements. All horizontal members were connected with dowels. FBDs with L-shaped support profiles have been installed in proper recesses left in the 12 solid 160-by-2500-by-8400 mm vertical panels or in the 16 solid 160-by-2100-by-8400 mm horizontal panels by acting from one side only. They have been provided with M16 bolts and with 50 mm long vertical slots. More details about the specimen, its connections and the description of the experimental campaign are available in [16,30,31]. Fig. 13 shows pictures of the structure provided with vertical panels (Fig. 13a) and horizontal panels (Fig. 13b).

The complete list of the cyclic and pseudo-dynamic tests performed on specimens with FBDs is reported in Table 3.

Several additional technological features have been explored during the tuning of the tests and adjustment of the connections. In particular, screws, nuts, and Belleville washers delivered in a first phase by the supplier were zinc-coated, as a normal practice for steel devices to improve their resistance to corrosion. The team of the ELSA laboratory found impossible to tighten the bolts, since they rotated before attaining the required level of torque given through the mechanical wrench. This was due to the different grip properties of zinc-coated steel, which has a lower friction coefficient with respect to standard burnished steel. All bolts and washers needed to be replaced. The protection to corrosion of the connection might be provided through painting after installation. The sliding surfaces are hidden and protected by the cover steel

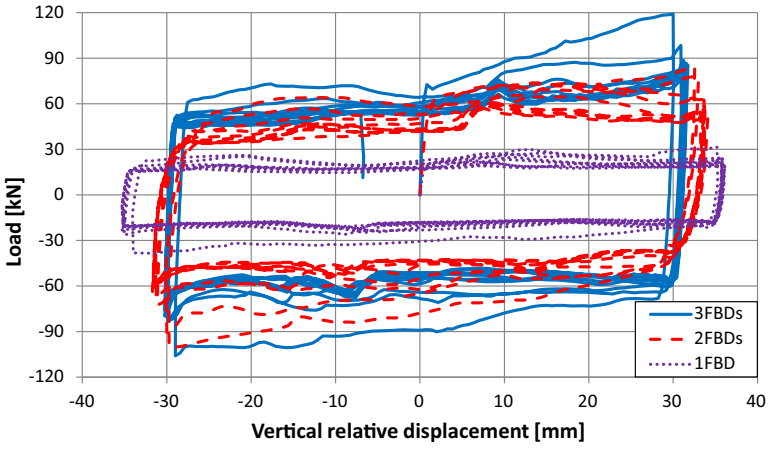

(a)

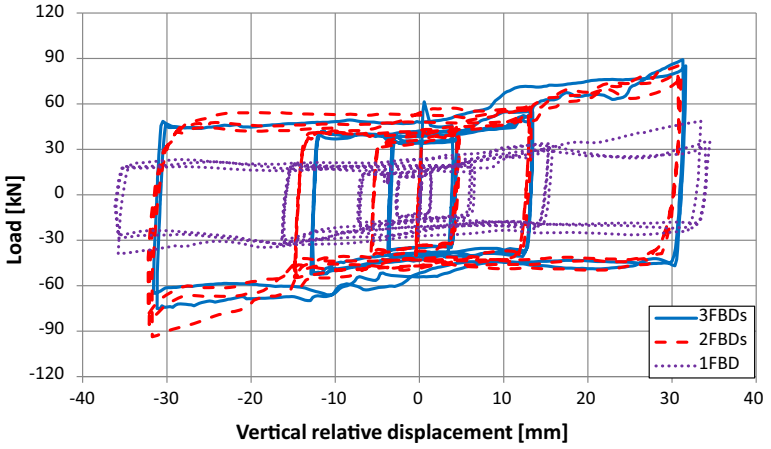

(b)

Fig. 12. Panel sub-assembly test results: load vs relative displacement of the panels provided with one, two, and three FBDs and tested with (a) protocol II (S-1, S-3 and S-5) and (b) protocol III (S-2, S-4 and S-6).

plate. It may be taken into account that the connections are designed to be installed in the inner side of the cladding panels, and therefore they are not supposed to be directly exposed to the external environment.

The cyclic tests are performed following a protocol with three displacement cycles repeated at the amplitudes of ±8,4–11,7–16, 4–23,0–32,1–45,0–63,0 mm. The maximum amplitude, corresponding to 0,9% of drift, is about 60% of the expected yielding drift of the columns.

In order to allow for large out-of-plane tolerances, horizontal slots have been milled on the angle support profiles at the panel side. The tightening of the bolts has been considered to be sufficient to avoid the activation of torsional rotations within the support pro-files. The load vs displacement cyclic diagram obtained with the first test performed with such a configuration, shown in Fig. 14, gave a slip threshold lower than the expected one, together with a slightly pinched behaviour. By observing the registered local motion of the connection, it has been noted that small torsional rotations of the support angle profiles occurred during the test. This did not occur in the sub-assembly tests, since symmetric profiles were used.

It has been then decided to weld the angle supports to the connecting plates embedded in the panel in order to keep them fixed in their position during the execution of further tests. This is still a feasible connection solution in practice, even if more onerous with respect to a bolted connection, since it can increase the construction cost (longer construction time and more human resources). The welded connection solution requires anyway a provisional bolting of the supporting angles to allow for the necessary adjustments of the device components, but in this case the bolts can be much smaller.

Pre-welding on the supporting angles of toothed plates and washers could have provided another feasible bolted solution able to prevent the torsional slides.

The results of the test performed on the specimen with all the connections adjusted in this way led to the attainment of a much larger base shear, as shown in Fig. 14, due to the achievement of the expected threshold slip load of the connections. No pinching has been observed with the welded support connection. For a correct interpretation of the results, it may be observed that the global behaviour of the structure is due to the superposition of the quasi rigid-plastic contribution of the FBDs and the elastic contribution of the frame.

The experimental campaign has been continued with this welded configuration of connections. Pseudo-dynamic tests were carried out by applying an accelerogram obtained from the Tolmezzo record artificially enriched in frequency content to fit the response spectrum provided by Eurocode 8 [8], as shown in Fig. 15.

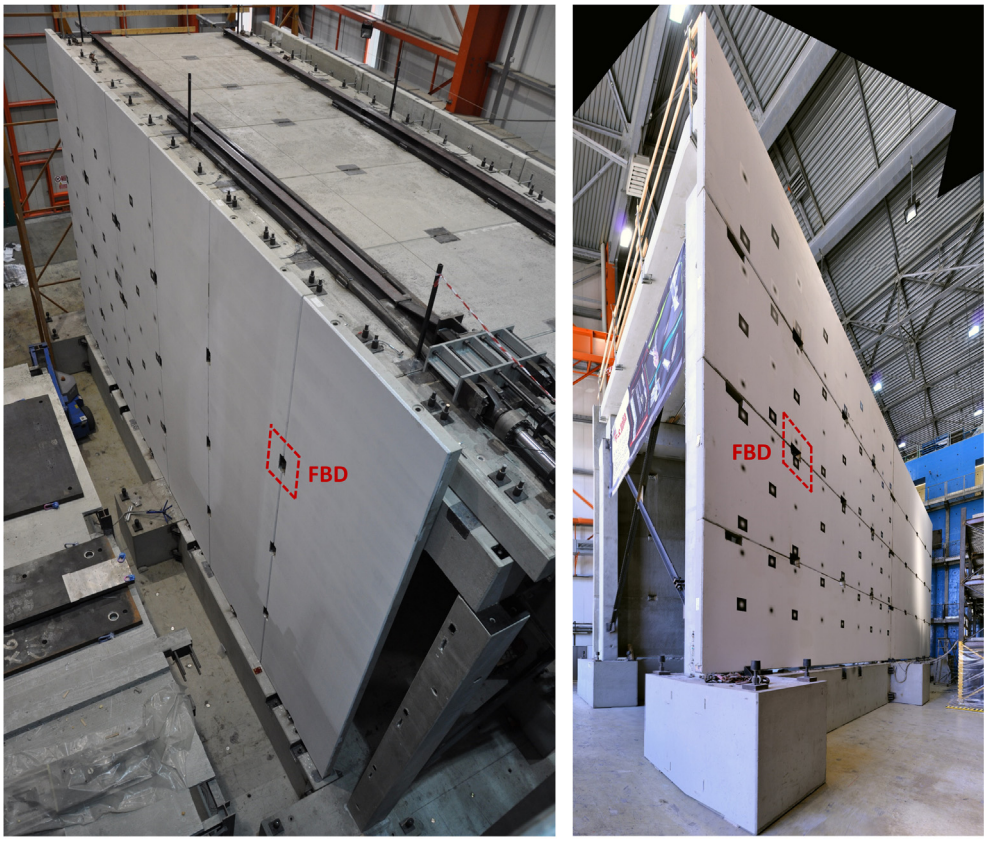

Fig. 13. Full-scale prototype of precast structure: (a) top view of the prototype provided with vertical panels and (b) bottom view of the prototype provided with horizontal panels (courtesy of M. Lamperti Tornaghi).

Table 3
List of the full scale prototype tests performed with FBDs.

Test ID	Panel type	Arrangement	No. of devices per panel side	Torque (Nm)	Test type
P-1	Vertical	Pendulum	3	220	Cyclic
P-2	Vertical	Pendulum	3	220	PsD 0,18 g
P-3	Vertical	Pendulum	3	220	PsD 0,36 g
P-4	Vertical	Pendulum	3	220	PsD 0,72 g
P-5	Vertical	Pendulum	3	220	PsD 1,00 g
P-6	Vertical	Pendulum	2	220	Cyclic
P-7	Vertical	Pendulum	2	220	PsD 0,36 g
P-8	Vertical	Pendulum	2	220	PsD 0,72 g
P-9	Vertical	Pendulum	1	220	Cyclic
P-10	Vertical	Pendulum	1	220	PsD 0,36 g
P-11	Vertical	Rocking	1	150	Cyclic
P-12	Vertical	Rocking	1	150	PsD 0,36 g
P-13	Horizontal	Swaying	2	220	Cyclic
P-14	Horizontal	Swaying	2	220	PsD 0,36 g
P-15	Horizontal	Swaying	2	220	PsD 0,54 g
P-16	Horizontal	Swaying	1	220	Cyclic
P-17	Horizontal	Swaying	1	220	PsD 0,36 g

Fig. 16 collects the base shear vs displacement diagrams obtained with pseudo-dynamic testing. The prototype has been subjected to accelerograms scaled at increasing $a_{g,max}$. The level of acceleration of the different tests was set on the basis of the blind predictions obtained by numerical simulations described in [16]. Fig. 16a shows the flexible response of the bare frame struc-

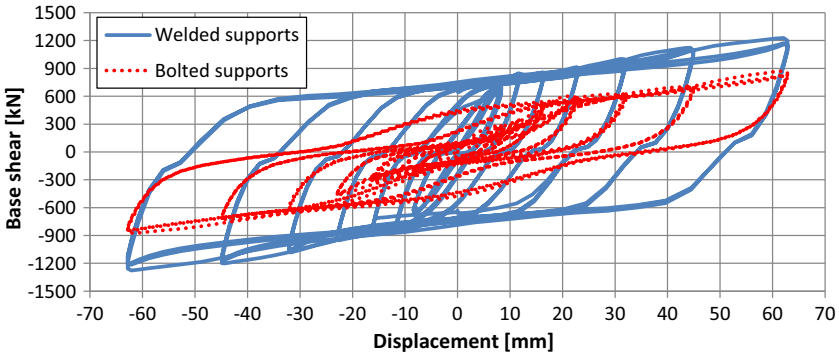

Fig. 14. Results from cyclic tests on prototype with 3 FBDs per joint: difference between bolted (preliminary test) and welded support profiles (test P-1).

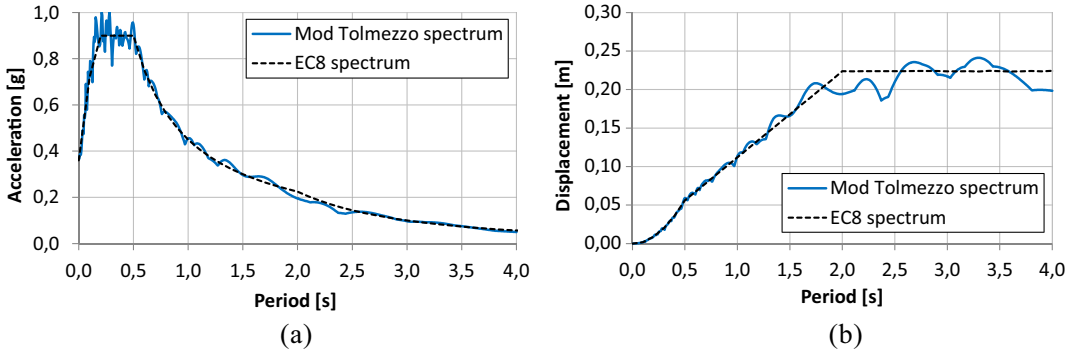

Fig. 15. Modified Tolmezzo accelerogram scaled at $a_{g,max}$ = 0,36 g: (a) acceleration response spectrum, (b) displacement response spectrum.

ture subjected to the modified Tolmezzo accelerogram scaled at the ULS $a_{g,max}$ of 0,36 g, with a maximum displacement of 220 mm and yielding and damage of the column bases. The proto-type with vertical panels linked at the structure with a pendulum arrangement, having pinned connections at the bottom and at the top along the central vertical line, and with three FBDs installed at each inter-panel joint has been subjected to an accelerogram scaled at a maximum $a_{g,max}$ of 1,00 g, corresponding to 2,8 times the design ULS of the frame structure. Even to this strong excita-tion, the frame structure responded elastically. The results (Fig. 16b) show that the hysteretic cycles of the overall structural system correspond to a large dissipation of energy concentrated into the FBDs. The maximum drift achieved is less than 88 mm, at which column base yielding is still not expected to occur. Fig. 17 shows the front view of the building and the detail of an FBD under maximum drift.

The column bases reached cracking, but they were far from the yielding of the reinforcing bars. The dissipative connections displaced with a maximum slide of 27 mm, which is about a half of their capacity (50 mm).

Fig. 16c shows the hysteretic cycles registered under an accelerogram scaled at $a_{g,max}$ = 0,36 g of the specimen with vertical panels linked with a rocking configuration, simply supported at the base edges on lateral shims and connected at the top with a vertical sliding connection. The specimen provided with a single FBD per interface shows a flag-shaped cyclic behaviour, due to the stiffening contribution of the concrete panels prior to their lifting up, after which they apply a constant elastic re-centring action. The dissipation of energy is sensibly lower and it is still related to the friction connectors only.

The experimental hysteretic cycles from the structure with horizontal panels and two FBDs per joint are shown in Fig. 16d with reference to the application of an accelerogram scaled at $a_{g,max}$ = 0,54 g. The panels are connected with a swaying arrangement, supported at the bottom on panel-to-column strong brackets and retained at the top with tie-back connections. The cyclic shape of the force-displacement cycles shows a highly dissipative behaviour.

During the tests with FBDs, all the structural members, including the panels, behaved elastically (the bare frame PsD test, whose results are shown in Fig. 16a, was carried out at the end of the experimental campaign). The column bases were cracked but not yielded. The very high amount of energy dissipated through the applied seismic actions has been all provided by the FBDs, that did not damage during their operation and were therefore in per-fect state at the end of the tests. As indicated by the local tests, also the brass sheets, that have been subject to large slippage, did not need replacement. This is confirmed by the fact that they provided similar responses throughout all the test series. Only the re-tightening of the connections has been executed at the end of each test. The maximum losses within all the bolts were not larger than 20 Nm, which is less than 10% of the initial torque. The permanent residual deformation of the structure, which is about 15 mm in the test with $a_{g,max}$ = 1,00 g, is simply related to the final position in which the FBDs have been found at the end of the excitation.

After the tests, the structure was re-centred by the action of the jacks. In real situations, if the precast frame structure remains in elastic field after an earthquake, as it was in the tested prototype, the frame itself provides a re-centring capacity which can be activated by simply untightening the FBDs. They have to be retightened after the structure moves back to its original position.

In practice, after the tests with FBDs the structure was ready to sustain additional strong earthquakes with large over-resources, granting a "full operability" performance level even after a seismic

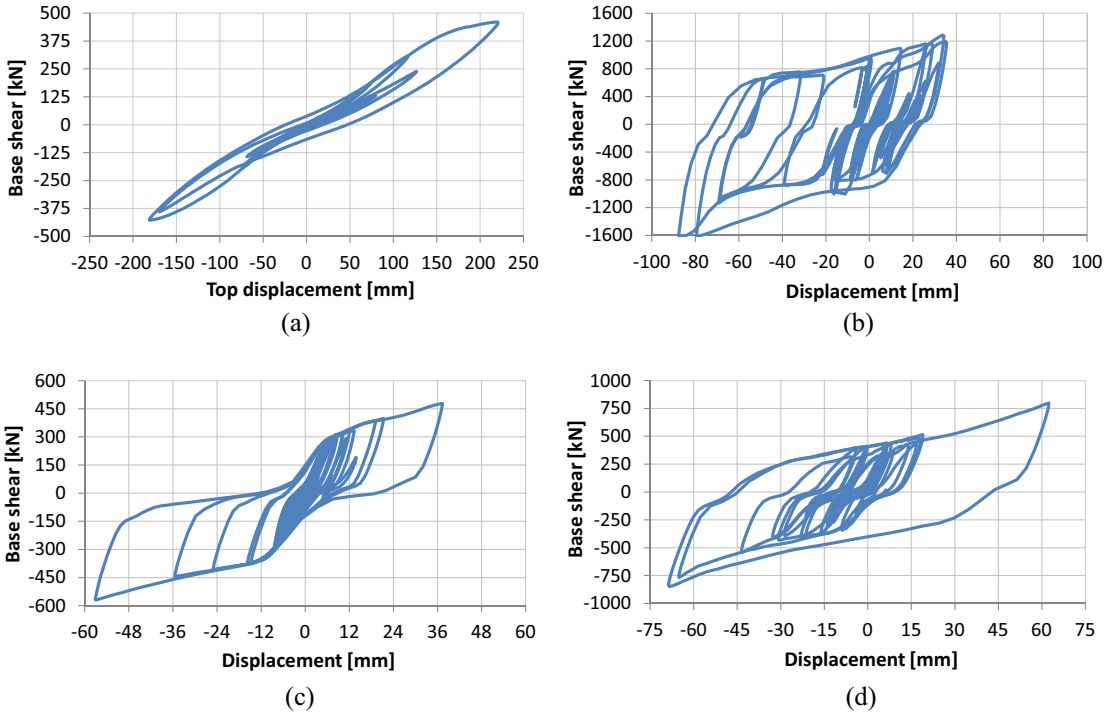

Fig. 16. Base shear vs top displacement diagrams from pseudo-dynamic tests on full-scale prototype: (a) bare frame ($a_{g,max}$ = 0,36 g); (b) test P-5 ($a_{g,max}$ = 1,00 g); (c) test P-12 ($a_{g,max}$ = 0,36 g) and (d) test P-15 ($a_{g,max}$ = 0,54 g).

action as strong as three times the ULS one of the bare frame structure. It is worth noting that structures are designed at ULS for the "no-collapse requirement" accepting heavy damages that could even lead to the necessity of demolition.

6. Design rules

The experimental tests showed that the FBDs may lead to different strength levels depending on complex random phenomena related to friction. Anyhow, the tendency of the cyclic behaviour of the tested connections can be identified as elastic-plastic, with an elastic stiffness within the range 40–60 kN/mm and a plastic branch up to the maximum allowed drift. The calculation of the plateau value to be used for the design of the device should be referred to three different strength parameters: (1) a mean value V_s associated to the static slip threshold, (2) a safe side lower value V, corresponding to the shear force reached after several cycles under dynamic friction, for the design of the overall structure, and (3) a safe side upper value $V + \Delta V$, associated with the maximum shear force that can occur, for the components of the connection to be proportioned according to capacity design. The geometrical properties of the plate are considered with reference to Fig. 3a, where d and e denote the vertical and horizontal distances, respectively, between the bolts.

The rotational equilibrium of the plate, subject to counteracting shear forces distanced by the eccentricity e, brings to inclined forces on the bolts. The vertical component is equal to half the acting shear, while the horizontal component is $Ve/(2d)$. The mean static slip load threshold V_s is obtained as follows:

$$V_s = N\frac{2\mu_s n k_s}{\sqrt{1+\frac{e^2}{d^2}}} \tag{1}$$

where μ_s is the static friction coefficient between brass and mild steel, that can be assumed equal to 0,51 [32], n is the number of sliding surfaces (standard connection has two sliding surfaces), k_s is a coefficient depending on the shape of the hole (for slots it can be assumed equal to 0,63 [33]).

The mean dynamic slip load threshold can be obtained by replacing μ_d to μ_s, where μ_d is the dynamic friction coefficient between brass and steel, that can be assumed equal to 0,44 [32].

The lower bound dynamic slip threshold force can be obtained by considering the oligo-cyclic losses due to bolt shortening for abrasion of brass surface. Including a factor φ that can be considered on experimental basis equal to 1,5 with the use of Belleville washers and to 3,0 with the use of traditional washers and, reversing the formulation, the design axial load N to be applied to a single bolt can be computed as follows:

$$N = \frac{V\varphi}{2\mu_d n k_s}\sqrt{1+\frac{e^2}{d^2}} \tag{2}$$

The experimental campaign shows that forces larger than the static threshold can occur during motion, and therefore an upper bound value higher than this limit should be adopted. Based on the experimental results, and on the safe side, the following equation is proposed in order to evaluate the maximum $V + \Delta V$ shear force that can occur during the motion:

$$V + \Delta V = \rho N\frac{2\mu_d n k_s}{\sqrt{1+\frac{e^2}{d^2}}} \tag{3}$$

where the coefficient ρ refers to the possible increase of the force and a recommended value is 1,6. This force could be used for the design of the other connections and members of the structure on the basis of the capacity of the FBD.

For a correct connection functioning, the bolts shall be able to slide through the slots without distorting them, otherwise sudden force peaks or blocking can arise. Specific checks should be made to this purpose.

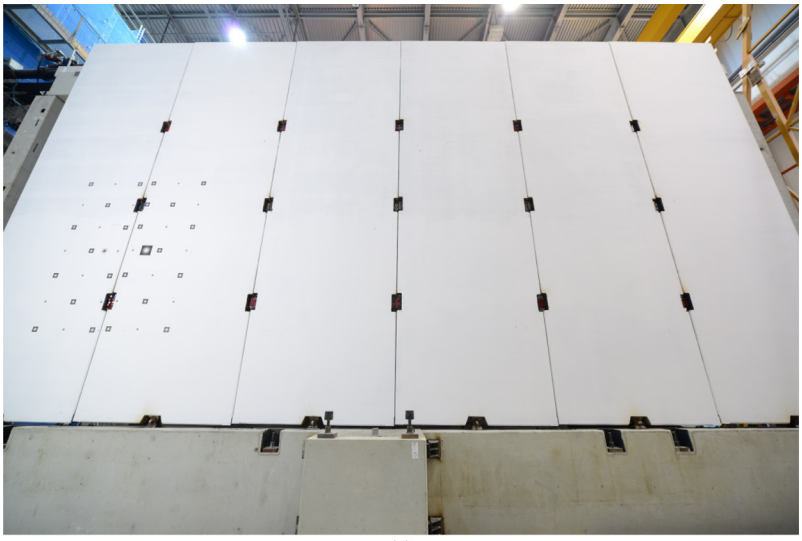

(a)

(b)

Fig. 17. Test P-5, maximum attained drift: (a) elevation view of the prototype and (b) detail of a FBD connection.

7. Conclusions

The experimental results presented in this paper showed that FBDs exhibit a quasi-rigid/pseudo-plastic behaviour with typical friction-type hysteresis and large energy dissipation capacity. The connection provided with brass sheets allows large cyclic stability, to which corresponds the possibility of re-use of the same connection after many large amplitude cycles. Moreover, it has been shown that the connection does not suffer from damage up to its maximum drift, which is a design parameter related to the length of the vertical slots of the connecting plates.

In structural assemblies where FBDs are used, residual displacements may remain after the loading sequence. Consequently, the release of the connections (untightening of the bolts) is needed for the re-centring of the structure. In addition, even though the brass sheets can be re-used after strong abrasion, the connections need to be re-tightened since abrasion causes losses of the bolt pre-tensioning. The pre-tensioning losses can be strongly reduced by using Belleville washers.

If a sufficient drift is assured by the slotted holes of the connections, the base shear of the structure induced by the seismic action is limited by the threshold force corresponding to the equilibrium of the panels subjected to the slip force of the friction devices. Moderate uncertainty is associated with the definition of the slip load threshold due to the friction mechanism. This has been taken into account in the definition of the proposed design rules.

The experimentation on a full scale prototype of precast structure proved that the use of FBDs can remarkably improve the seismic performance due to the relevant added hysteretic damping and consequent reduction of structural drifts under controlled forces. This allows to protect the frame structure from yielding.

The FBD dissipative system of connections shows very promising features for fruitful applications in seismic design of precast structures. The effectiveness of the earthquake resisting system, that employs the wall panels with dissipative mutual connections as bracing elements of the frame structure, depends on both the plan layout of the building and roof diaphragm action. For the type of tested structure, with only one transverse bay that shares its mass on the two lateral bracing walls, the higher effectiveness of the dissipative devices could be attained. For other plan configurations, the actual functioning of the system should be evaluated case by case considering the specific arrangement of the cladding elements.

Acknowledgements

The work presented in this paper has been funded by the European Commission within the FP7-SME-2011 SAFECLADDING

research project (Grant agreement No. 314122, 2012), and partially by the Italian Department of Civil Protection (DPC) and the Italian Laboratories University Network of Earthquake Engineering (ReLUIS) within the research program DPC-ReLUIS 2014-2016. The financial supports of the funding institutions are gratefully acknowledged. Gratitude and appreciation are expressed to Marco Lamperti Tornaghi, Silvia Bianchi, Giulia Marelli, Giulia Mariani Orlandi and Alessandro Rocci for their contributions to the execution of the tests performed at Politecnico di Milano. The experimental tests on the full scale prototype have been performed at the European Laboratory of Structural Assessment of the Joint Research Centre (JRC) of the European Commission. Special thanks are due to all members of the JRC team, particularly to Paolo Negro, Javier Molina, Pierre Pegon, and Marco Lamperti Tornaghi.

References

[1] Biondini F, Toniolo G. Probabilistic calibration and experimental validation of seismic design criteria for one storey concrete frames. J Earth Eng 2009;13 (4):426–62.
[2] Biondini F, Toniolo G, Tsionis G. Capacity design and seismic performance of multi-storey precast structures. Eur J Environ Civ Eng 2010;14(1):11–28.
[3] Kramar M, Isakovic T, Fischinger M. Seismic collapse risk of precast industrial buildings with strong connections. Earthq Eng Struct Dyn 2012;39(8):847–68.
[4] Psycharis IN, Mouzakis HP. Shear resistance of pinned connections of precast members to monotonic and cyclic loading. Eng Struct 2012;41:413–27.
[5] Negro P, Bournas DA, Molina J. Pseudodynamic tests on a full-scale 3-storey precast concrete building: global response. Eng Struct 2013;57:594–608.
[6] Yuksel E, Karadogan FH, Bal EI, Ilki A, Bal A, Inci P. Seismic behavior of two exterior beam–column connections made of normal-strength concrete developed for precast construction. Eng Struct 2015;99:157–72.
[7] Dal Lago B, Toniolo G, Lamperti Tornaghi M. Influence of different mechanical column-foundation connections on the seismic performance of precast structures. Bull Earthq Eng 2016;14(12):3485–508.
[8] CEN-EN 1998-1. Eurocode 8: Design of structures for earthquake resistance – Part 1: General rules, seismic actions and rules for buildings. Brussels, Belgium: European Committee for Standardization; 2004.
[9] Menegotto M. Experiences from L'Aquila 2009 earthquake. 3rd fib Congress, Washington DC, USA, 29 May – 2 June, 2010.
[10] Toniolo G, Colombo A. Precast concrete structures: the lesson learnt from L'Aquila earthquake. Struct Concr 2012;13(2):73–83.
[11] Savoia M, Mazzotti C, Buratti N, Ferracuti B, Bovo M, Ligabue V, et al. Damages and collapses in industrial precast buildings after the Emilia earthquake. Ingegneria Sismica 2012;29(2–3):120–31.
[12] Bournas D, Negro P, Taucer F. Performance of industrial buildings during the Emilia earthquakes in Northern Italy and recommendations for their strengthening. Bull Earthq Eng 2013;12(5):2383–404.
[13] Magliulo G, Ercolino M, Petrone C, Coppola O, Manfredi G. Emilia earthquake: the sesmic performance of precast RC buildings. Earthq Spectra 2014;30 (2):891–912.
[14] Colombo A, Negro P, Toniolo G. The influence of claddings on the seismic response of precast structures: the Safecladding project. 2nd European Conference on Earthquake Engineering and Seismology, Istanbul, Turkey, August 25–39, 2014; paper No. 1877.
[15] Biondini F, Dal Lago B, Toniolo G. Role of wall panel connections on the seismic performance of precast structures. Bull Earthq Eng 2013;11(4):1061–81.
[16] Dal Lago B. Seismic performance of precast structures with dissipative cladding panel connections [Ph.D. thesis]. Politecnico di Milano, Milan, Italy: Department of Civil and Environmental Engineering; 2015.
[17] Schultz AE, Magana RA, Tadros MK, Huo X. Experimental study of joint connections in precast concrete walls. 5th U.S. NCEE, Chicago, USA, July 10–14, 1994;2:579–587.
[18] Tyler RG. Damping in building structures by means of PTFE sliding joints. Bull New Zealand Soc Earthq Eng 1977;10(3):139–42.
[19] Grigorian CE, Yang TS, Popov EP. Slotted bolted connection energy dissipators. Earthq Spectra 1987;9(3):491–504.
[20] Pall AS. Friction Damped Connections for Precast Concrete Cladding. International Symposium on Architectural Precast Concrete Cladding – Its Contribution to Lateral Resistance of Buildings, Chicago, USA, November 8–9, 1989;300–310.
[21] Cherry S, Filiatrault A. Seismic response control of building using friction dampers. Earthq Spectra 1993;9(3):447–66.
[22] Mualla IH. Experimental and numerical evaluation of a novel friction damper device [Ph.D. thesis]. Kongens Lingby, Denmark: Department of Structural Engineering and Materials, Technical University of Denmark; 1999.
[23] Mualla IH, Nielsen LO, Belev B, Liao WI, Loh CH, Agrawal A. Numerical predictions of shaking table tests on a full scale friction-damped structure. 12th European Conference on Earthquake Engineering, London, UK, September 9–13, 2002; paper No. 109.
[24] Martinelli P, Mulas MG. An innovative passive control technique for industrial precast frames. Eng Struct 2010;32:1123–32.
[25] Valente M. Improving the seismic performance of precast buildings using dissipative devices. 2nd International Conference on Rehabilitation and Maintenance in Civil Engineering, Solo, Indonesia, March 8–10, 2013;54:795–804.
[26] Ferrara L, Felicetti R, Toniolo G, Zenti C. Friction dissipative devices for cladding panels in precast buildings. Eur J Environ Civ Eng 2011;15 (9):1319–38.
[27] Biondini F, Dal Lago B, Toniolo G. Experimental and numerical assessment of dissipative connections for precast structures with cladding panels. 2nd European Conference on Earthquake Engineering and Seismology, Istanbul, Turkey, August 25–39, 2014;paper No. 2168.
[28] Biondini F, Dal Lago B, Toniolo G. Experimental tests on dissipative cladding connection systems of precast structures. 16th World Conference on Earthquake Engineering, Santiago, Chile, January 9–13, 2017;paper No. 933.
[29] Guran A, Pfeiffer F, Popp K. Dynamic with friction; modelling, analysis and experiment: part I. USA: World Scientific Publishing Co Pte Ltd; 1996.
[30] Negro P, Lamperti Tornaghi M. Seismic response of precast structures with vertical cladding panels: the SAFECLADDING experimental campaign. Eng Struct 2017;132:205–28.
[31] Toniolo G, Dal Lago B. Conceptual design and full-scale experimentation of cladding panel connection systems of precast buildings. Earthq Eng Struct Dyn 2017. http://dx.doi.org/10.1002/eqe.2918.
[32] Quayle JP. Kempe's engineers' year books. UK: Morgan-Grampian Ltd.; 1980.
[33] CEN-EN 1993-1-8. Eurocode 3: design of steel structures – Part 8: design of joints. Brussels, Belgium: European Committee for Standardization; 2005.